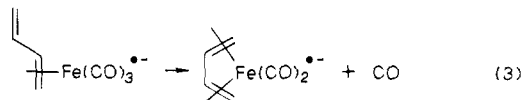
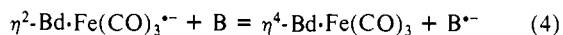


produce the $\eta^4\text{-Bd}\cdot\text{Fe}(\text{CO})_2^{\bullet-}$ ion. It is envisaged that the uncoordinated butadiene double bond in the molecular ion recoordinates to the metal and displaces a CO molecule as shown in reaction 3. Since electron capture by $\eta^4\text{-Bd}\cdot\text{Fe}(\text{CO})_3$ results in



cleavage of an Fe-alkene bond rather than an Fe-CO bond, it appears that reaction 3 must be endothermic and is driven by the entropy gain of the dissociation (3). Measurements of the rate of (3) at higher temperatures led, via an Arrhenius plot, to an activation energy, $E_3 \approx 20$ kcal/mol. Further experiments¹¹ involving the equilibrium 3 indicated that E_3 is close to the enthalpy change ΔH_3 .

The free energy of electron attachment to $\eta^4\text{-Bd}\cdot\text{Fe}(\text{CO})_3$, $\Delta G_a^\circ[\eta^4\text{-Bd}\cdot\text{Fe}(\text{CO})_3]$, was determined by measuring the equilibrium constant for electron-transfer reaction 4, K_4 , where B corresponds to reference molecules nitrobenzene, *p*-fluoronitrobenzene, or *m*-fluoronitrobenzene. The free energies for electron attachment to these reference molecules, $\Delta G_a^\circ(\text{B})$, have been determined previously to be -22.8, -25.0, and -27.7 kcal mol⁻¹, respectively. Upon determination of ΔG_4° for each electron-transfer equilibrium according to eq 5, $\Delta G_a^\circ[\eta^4\text{-Bd}\cdot\text{Fe}(\text{CO})_3]$ was calculated by inserting the appropriate values of ΔG_4° and $\Delta G_a^\circ(\text{B})$ into eq 6. Figure 1 shows a pair of ion time profiles



$$\Delta G_4^\circ = -RT \ln K_4 \quad (5)$$

$$\Delta G_a^\circ[\eta^4\text{-Bd}\cdot\text{Fe}(\text{CO})_3] = \Delta G_a^\circ(\text{B}) - \Delta G_4^\circ \quad (6)$$

obtained during these experiments. In this particular case $\eta^2\text{-Bd}\cdot\text{Fe}(\text{CO})_3^{\bullet-}$ was the predominant ion present shortly after the electron pulse, but its intensity decreased steadily due to electron transfer to *m*-fluoronitrobenzene until, after approximately 2 ms, equilibrium was achieved as evidenced by the parallel ion plots, and K_4 was calculated from the constant ion ratio observed beyond this point. A series of experiments where P_A/P_B was progressively changed by a factor of 10 led to K_4 values which were independent of the pressure ratio as expected from eq 5. From the average value of K_4 for each reference compound, ΔG_4° was calculated to be +2.5, +0.4, and -2.4 kcal mol⁻¹, respectively, for electron transfer from $\eta^2\text{-Bd}\cdot\text{Fe}(\text{CO})_3^{\bullet-}$ to nitrobenzene, *p*-fluoronitrobenzene, and *m*-fluoronitrobenzene. These values lead via eq 6 to $\Delta G_a^\circ[\eta^4\text{-Bd}\cdot\text{Fe}(\text{CO})_3] = -25.3, -25.4, \text{ and } -25.3$ kcal mol⁻¹, respectively, and an overall mean of -25.3 kcal mol⁻¹.

An interesting feature of the time profiles shown in Figure 1 is the very slow approach to equilibrium which is evident in the first 2 ms. This slow approach to equilibrium corresponds to a rate of electron transfer from $\eta^2\text{-Bd}\cdot\text{Fe}(\text{CO})_3^{\bullet-}$ to *m*-fluoronitrobenzene of only 5×10^{-12} cm³ molecule⁻¹ s⁻¹, even though this reaction is exoergic by 2.4 kcal mol⁻¹. Since exoergic electron-transfer reactions in the gas phase frequently proceed at the collisionally determined maximum rate of $\approx 2 \times 10^{-9}$ cm³ molecule⁻¹ s⁻¹,⁵ it is evident that electron transfer from $\eta^2\text{-Bd}\cdot\text{Fe}(\text{CO})_3^{\bullet-}$ to *m*-fluoronitrobenzene is highly inefficient. This is probably associated with the large difference in structure between $\eta^2\text{-Bd}\cdot\text{Fe}(\text{CO})_3^{\bullet-}$ and $\eta^4\text{-Bd}\cdot\text{Fe}(\text{CO})_3$. Slow rates of electron transfer caused by large structural changes have been identified previously.¹²

More elaborate measurements including variable temperatures, currently in progress,¹¹ indicate, via van't Hoff plots of reaction 4, that the ΔS_2° value for the electron capture (2) is consistent with the expected increased freedom of internal rotation in the $\eta^2\text{-Bd}\cdot\text{Fe}(\text{CO})_3^{\bullet-}$ product ion. Details of these and additional related results will be given in a forthcoming publication.¹¹

(11) Dillow, G. W.; Kebarle, P. manuscript in preparation.

(12) Grimrud, E. P.; Chowdhury, S.; Kebarle, P. J. *Chem. Phys.* **1985**, *104*, 83, 1059. Chowdhury, S.; Kebarle, P. *Chem. Phys.* **1986**, *85*, 4989.

Proton NMR Detection of Long-Range Heteronuclear Multiquantum Coherences in Proteins: The Complete Assignment of the Quaternary Aromatic ¹³C Chemical Shifts in Lysozyme

Donald G. Davis

Laboratory of Molecular Biophysics
National Institute of Environmental Health
P. O. Box 12233
Research Triangle Park, North Carolina 27709

Received March 3, 1989

The development of reverse detection methods¹ has stimulated a renewed interest in ¹³C NMR of macromolecules.^{2,3} In these experiments ¹³C chemical shifts are determined indirectly by detecting the influence of evolving heteronuclear multiquantum coherences on the magnetization of protons scalar coupled to ¹³C. Although maximum sensitivity is obtained for carbons directly bonded to protons, experiments for ¹H detection of multibond heteronuclear correlations have been developed,⁴⁻⁷ but the sensitivity is less and applications have been limited to small molecules or to isotopically enriched macromolecules.^{8,9} It might appear therefore that ¹³C NMR studies of macromolecules using ¹H detection complement those using direct ¹³C detection, where attention was focused, of necessity, on nonprotonated quaternary carbons.¹⁰ This communication demonstrates to the contrary that the shifts of quaternary carbons in the aromatic rings of proteins can be obtained via ¹H detection with almost the same sensitivity as the protonated carbons and thus be used to completely assign the ¹H¹³C 2D spectra of these carbons in a 4.4 mM solution of lysozyme (MW = 14 300). Our results extend and refine those of Allerhand and co-workers¹⁰ who used chemical modification and titration schemes to make assignments. Of greater significance however is the improvement in sensitivity and attendant reduction in materials and time required to solve the assignment problem.

This experiment succeeds for several reasons. First, almost all the quaternary aromatic carbons in proteins are coupled to ring protons through three-bond trans couplings, that are uniformly about 8 Hz.¹¹ Secondly, sensitivity is limited principally by proton T_2 's. Consequently long-range multiquantum states can be optimally prepared ($I_\alpha S_\beta \sin(\pi J \Delta)$; $\alpha, \beta \neq z$) without serious attenuation by relaxation ($\exp(-\Delta/T_2)$). Thirdly, several peaks in the 2D spectra are multiply correlated, while the one-bond correlations are suppressed (vide infra), thus facilitating the assignment problem. Finally, for lysozyme, all the protonated aromatic ¹³C's and their attached ¹H's have been assigned.^{3,12}

For this particular application, we used the HMQC¹³ sequence: $90^\circ_x(\text{H})-\Delta-90^\circ_\phi(^{13}\text{C})-t_1/2-180^\circ_x(\text{H})-t_1/2-90^\circ_x(^{13}\text{C})-\Delta-[-\text{acquire}(t_2)]$ with ¹³C decoupling. In addition to providing max-

- (1) Griffey, R. H.; Redfield, A. G. *Quart. Rev. Biophys.* **1987**, *19*, 51.
- (2) Wagner, G.; Brühwiler, D. *Biochemistry* **1986**, *15*, 5839.
- (3) Sklenar, V.; Bax, A. *J. Magn. Reson.* **1987**, *71*, 379.
- (4) Bax, A.; Summers, M. F. *J. Am. Chem. Soc.* **1986**, *108*, 2093.
- (5) Bermel, W.; Griesinger, C.; Kessler, H.; Wagner, K. *Magn. Reson. Chem.* **1987**, *25*, 325.
- (6) Bax, A.; Marion, D. *J. Magn. Reson.* **1989**, *78*, 186.
- (7) Davis, D. G. *J. Magn. Reson.* **1989**, *83*, 212.
- (8) Westler, W. M.; Kainosho, M.; Nagao, H.; Tomonaga, N.; Markley, J. L. *J. Am. Chem. Soc.* **1988**, *110*, 4093.
- (9) Bax, A.; Sparks, S. W.; Torchia, D. A. *J. Am. Chem. Soc.* **1988**, *110*, 7926.
- (10) Allerhand, A. *Methods Enzymol.* **1979**, *61*, 458 and references therein.
- (11) Memory, J. D.; Wilson, N. K. *NMR of Aromatic Compounds*; J. Wiley and Sons: New York, 1982; Chapter 5. The cis coupling between Trp-H₃ and -C₇ is apparently small (<3 Hz) but fortunately ²J between Trp-H₃₁ and -C₇ is ca. 6 Hz. All other geminal ring C-H ²J's here are negligibly small (<3 Hz).
- (12) Redfield, C.; Poulson, F. M.; Dobson, C. M. *Eur. J. Biochem.* **1982**, *128*, 527.
- (13) Bax, A.; Griffey, R. H.; Hawkins, B. L. *J. Magn. Reson.* **1983**, *55*, 301. For absorption mode spectra,^{3,13} $\phi = x, y, -x, -y$, with odd and even acquisitions stored in separate blocks of memory and the FID's alternately added and subtracted in each block (i.e., receiver phase = +, +, -, -).

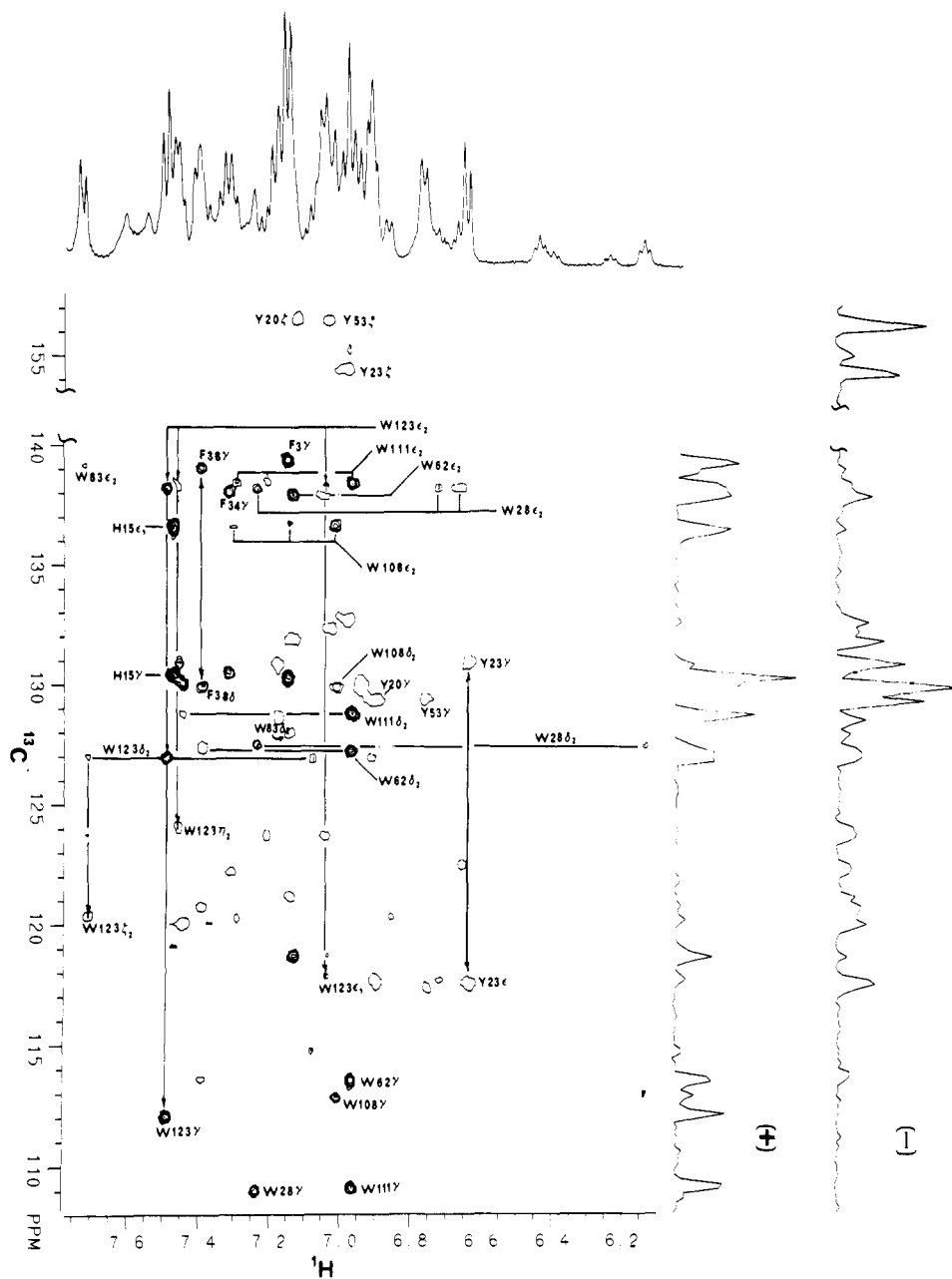


Figure 1. Absorption mode,¹⁸ long-range $^1\text{H}\{^{13}\text{C}\}$ correlation spectrum of the aromatic region of lysozyme (Boehringer Mannheim; 25 mg/0.4 mL) in D_2O , pH 7 and 47 °C, recorded at 500 MHz on a GNS500 spectrometer with the HMQC sequence¹³ with $\Delta = 50$ ms. The peaks drawn with filled (positive) contours indicate long-range correlations of ^{13}C with protons having triplet or singlet multiplicity, while the open (negative) contours indicate correlations with proton doublets. The projections of these peaks onto the ^{13}C axis are shown at the right and indicated by (+) and (-). Not shown are cross peaks between His(15)- C_γ (130.4 ppm) and $-\text{C}_{62}$ (119.4 ppm) and the $-\text{H}_{61}$ at 8.85 ppm. The initial (t_1 , t_2) data set consisted of $2 \times 96 \times 1024$ real points acquired over a period of 21 h with acquisition times of 15.3 ms (t_1) and 205 ms (t_2), a 1.2-s delay between acquisitions and 2×260 acquisitions per t_1 increment. Prior to Fourier transformation, a 7-Hz Gaussian broadening was applied in the t_2 dimension, and in t_1 , a 24-Hz broadening and zero fill to 256 points. To minimize phasing difficulties in F_1 due to ^{13}C precession during the finite pulse intervals ($90^\circ(^1\text{H}) = 24 \mu\text{s}$; $90^\circ(^{13}\text{C}) = 40 \mu\text{s}$) a fixed delay of $16 \mu\text{s}$ was inserted in the t_1 interval, and the t_1 files were right shifted by one data point before transformation.

imum resolution, it has another useful feature. Namely, Δ can be set (~ 50 ms) so that one achieves multiplet labeling^{14,15} in the sense that the peak intensities are positive if they represent correlations with protons having triplet or singlet multiplicity, while they are negative if correlated with proton doublets. Together, multiplet labeling and the multiple correlation of peaks reduce ambiguities and have enabled us to correct some previous misassignments.¹⁶ Also with $\Delta = 50$ ms, the one-bond correlations are suppressed by ^1H - ^{13}C dipolar transverse relaxation.

The long-range $^1\text{H}\{^{13}\text{C}\}$ correlation spectrum for the aromatic side chains of lysozyme is shown in Figure 1. For clarity, only those peaks assigned to quaternary carbons are completely identified,¹⁷ but a few examples of multiple connectivity are illustrated. Most of the expected peaks in the aromatic region are visible, while others can be seen at deeper contours. Some however are missing entirely; the most notable being the Trp(63) $\text{H}_{\beta 1}$ - C_γ cross peak which, by a process of elimination and reference to previous studies,¹⁰ should be found at ca. 110 ppm. Also missing or present at low intensities are some of the peaks for the Trp- $\text{C}_{\beta 2}$

(14) Campbell, I. D.; Dobson, C. M.; Williams, R. J. P.; Wright, P. E. *FEBS Lett.* **1975**, *57*, 96.

(15) Davis, D. G. *J. Magn. Reson.* **1989**, *82*, 640.

(16) The ^{13}C assignments (ref 3) for the pair Trp(62)- $\text{C}_{\beta 1}$ and Trp(62)- $\text{C}_{\beta 2}$ as well as for Phe(3)- C_β and Phe(3)- C_γ should be reversed.

(17) Labeling follows the IUPAC-IUB convention: *Eur. J. Biochem.* **1970**, *17*, 1993.

(18) Müller, L.; Ernst, R. R. *Mol. Phys.* **1979**, *38*, 963.

and $-C_{63}$'s. Since all the relevant coupling constants are essentially equal, the variations in peak intensities may reflect differences in 1H T_2 's which in turn are sensitive to differences in modes of internal motion. Indeed our failure to observe the Trp(63)- C_{γ} - $H_{\delta 1}$ cross peak is not unexpected, for it is known that the Trp(63)- $H_{\delta 1}$ resonance is broadened by conformational exchange.¹²

In summary the natural abundance ^{13}C shifts of the non-protonated aromatic carbons in proteins can be readily determined by 1H detection of long-range heteronuclear correlations provided the 1H T_2 's are long enough to preserve multiplet structure in the 1H spectra. By taking advantage of the coupling properties of aromatic spin systems and choosing delay times appropriately, one can also impose a pattern on the 2D spectra that permits partial assignments without a priori assumptions about chemical shifts. Moreover if the proton assignments are known, one can, as demonstrated here for lysozyme, assign the quaternary aromatic carbon spectra completely without additional experimentation.

Supplementary Material Available: Fully annotated versions of the 2D long-range and one-bond $^1H\{^{13}C\}$ correlation spectra of the aromatic region of lysozyme (Figures S1 and S2) and a table of ^{13}C chemical shifts (4 pages). Ordering information is given on any current masthead page.

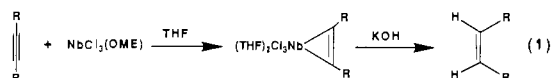
A Regioselective Synthesis of 2,3-Disubstituted-1-naphthols. The Coupling of Alkynes with 1,2-Aryldialdehydes Promoted by $NbCl_3(DME)$

Jack B. Hartung, Jr., and Steven F. Pedersen*

Department of Chemistry, University of California
Berkeley, California 94720

Received February 23, 1989

Recently we described a new synthesis of 2-amino alcohols via the reductive coupling of aldimines with aldehydes or ketones promoted by the niobium(III) reagent, $NbCl_3(DME)$.¹ Low-valent, early transition-metal halides, including some previously reported niobium(III) compounds are known to react with alkynes to give alkyne complexes.² $NbCl_3(DME)$ behaves in a similar fashion as shown in eq 1.³ Hydrolysis of these complexes with



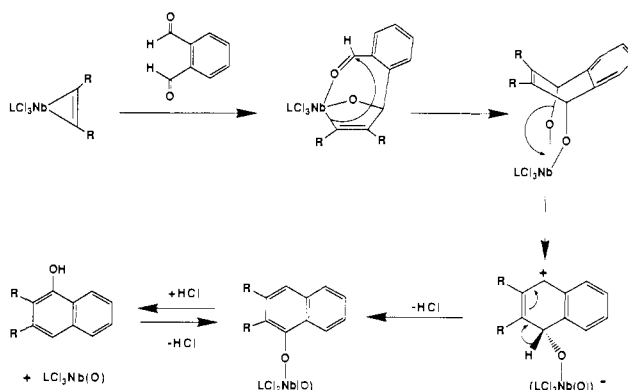
aqueous potassium hydroxide yields *cis*-olefins, indicating that such species may function as a source of 1,2-alkene dianions.^{2c,4} Herein, we report a convenient and regioselective synthesis of 2,3-disubstituted-1-naphthols via the coupling of alkynes with 1,2-aryldialdehydes promoted by $NbCl_3(DME)$.

Niobium alkyne complexes are generated in situ by adding the alkyne to $NbCl_3(DME)$ in tetrahydrofuran and gently refluxing the solution for 10–14 h. These species may also be formed at room temperature employing longer reaction times. Addition of phthalic dicarboxaldehyde to complexes derived from symmetrical alkynes ($R = R'$, eq 1) leads to, after workup, the 1-naphthol products shown in Table I (entries 1–2). A mechanism that accounts for these products is proposed in Scheme I. Stepwise

Table I

entry	R	R'	W	A:B	yield (%)
1	Ph	Ph	H		87
2	<i>n</i> -Pr	<i>n</i> -Pr	H		81
3	4-MeOPh	Ph	H	3:1	61
4	Me	<i>i</i> -Pr	H	2:1	75
5	Me	<i>t</i> -Bu	H	>99:1	60
6	Me	Me ₃ Si	H	>99:1	70
7	Ph	(<i>t</i> -Bu)Me ₂ Si	H	>99:1	83
8	Ph	(<i>t</i> -Bu)Me ₂ Si	OMe	>99:1	66
9	TBDMSO(CH ₂) ₂	Me ₃ Si	H	>99:1	62
10		Me ₃ Si	H	>99:1	57
11	Ph	Me ₃ Si		>99:1	53

Scheme I

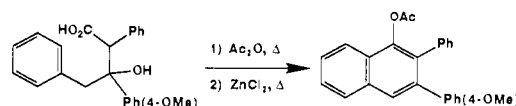


insertion of each formyl group into a metal-carbon bond would lead to the cyclic 1,4-dialkoxy-1,4-dihydronaphthalene intermediate. Ionization of one of the carbon-oxygen bonds followed by proton loss then leads to product.⁵ When (4-methoxyphenyl)-phenylacetylene is used in this reaction a 3:1 mixture of isomeric naphthols is obtained (entry 3). The major isomer (established by independent synthesis of the minor isomer⁶) is that predicted from the mechanism proposed in Scheme I where the 4-methoxyphenyl group is better able to stabilize the developing positive charge than the unsubstituted phenyl ring. We have also confirmed by 1H NMR experiments⁷ that naphthol (or naphthoxide) is generated during the course of the reaction (i.e., before workup) as depicted in Scheme I. The driving forces behind this reaction are formation of an aromatic ring and a niobium-oxo group.

When trialkylsilyl-substituted alkynes are employed, good yields of a single regioisomer, namely the 3-(trialkylsilyl)-2-alkyl (or aryl)-1-naphthols, are obtained. The regiochemical assignments for entries 6 and 7 were established by preparing 2-methyl-⁸ and 2-phenyl-1-naphthol,⁹ respectively, by removal of the trialkylsilyl group (CF_3CO_2H ¹⁰). The well-established synthetic utility of aryltrialkylsilanes¹¹ makes these products particularly attractive

(5) Analogous to acid-catalyzed dehydration of *cis*-1,4-dihydroxy-1,4-dihydronaphthalene: Jeffrey, A. M.; Yeh, H. J. C.; Jerina, D. M. *J. Org. Chem.* **1974**, *39*, 1405.

(6) Mondeshka, D. M.; Angelova, I. G. *Rev. Roumaine de Chimie* **1974**, *19*, 1759.



(7) Reactions were carried out in NMR tubes with purified alkyne complexes.

(8) An authentic sample was obtained from Aldrich Chemical Company.

(9) Barton, D. H. R.; et al. *J. Chem. Soc., Perkin Trans. 1* **1985**, 2657.

(10) Diercks, R.; Vollhardt, K. P. C. *J. Am. Chem. Soc.* **1986**, *108*, 3150.

(1) Roskamp, E. J.; Pedersen, S. F. *J. Am. Chem. Soc.* **1987**, *109*, 6551.

(2) (a) Walborsky, E. C.; Wigley, D. E.; Roland, E.; Dewan, J. C.; Schrock, R. R. *Inorg. Chem.* **1987**, *26*, 1615. (b) Cotton, F. A.; Roth, W. *J. Inorg. Chim. Acta* **1984**, *85*, 17. (c) Theopold, K. H.; Holmes, S. J.; Schrock, R. R. *Angew. Chem., Int. Ed. Engl.* **1983**, *22*(12), 1010. (d) Cotton, F. A.; Hall, W. T. *Inorg. Chem.* **1981**, *20*, 1285. (e) Cotton, F. A.; Hall, W. T. *Inorg. Chem.* **1980**, *19*, 2352. (f) Greco, A.; Pirinoli, F.; Dall'Asta, G. *J. Organomet. Chem.* **1973**, *60*, 115.

(3) Details of these complexes will be described elsewhere.

(4) For examples of the relatively rare and unstable 1,2-dilithioalkenes, see: (a) Maercker, A.; Theis, M. *Top. Curr. Chem.* **1987**, *138*, 1. (b) Maercker, A.; Graule, T.; Girreser, U. *Angew. Chem., Int. Ed. Engl.* **1986**, *25*, 167. (c) Levin, G.; Jagur-Grodzinski, J.; Szwarc, M. *J. Am. Chem. Soc.* **1970**, *92*, 2268.